Article ID: 1006-8775(2022) 03-0297-11

A Comparative Analysis of Chemical Properties and Factors Impacting Spring Sea Fog over the Northwestern South China Sea

HAN Li-guo (韩利国)[1, 2, 3], XU Feng (徐 峰)[1, 2, 3], XU Jian-jun (徐建军)[1, 2, 4],
LI Ya-jie (李雅洁)[1], CHAI Bo-yu (柴博语)[1], LÜ Jing-jing (吕晶晶)[5]
(1. College of Ocean and Meteorology/ South China Sea Institute of Marine Meteorology (SIMM), Guangdong Ocean University, Zhanjiang, Guangdong 524088 China; 2. CMA-GDOU Joint Laboratory for Marine Meteorology, Guangdong Ocean University, Zhanjiang, Guangdong 524088 China; 3. Key Laboratory of Climate, Resources and Environment in Continental Shelf Sea and Deep Sea of Department of Education of Guangdong Province, Guangdong Ocean University, Zhanjiang, Guangdong 524088 China; 4. Shenzhen Institute of Guangdong Ocean University, Shenzhen, Guangdong 518120 China; 5. Key Laboratory for Aerosol-Cloud-Precipitation of China Meteorological Administration, Nanjing University of Information Science and Technology, Nanjing 210044 China)

Abstract: In the present study, we analyzed the chemical properties and factors impacting the sea fog water during two sea fog events over the northwestern South China Sea in March 2017, and compared our results with those of other regions. The sea fog water during these two events were highly acidic and their average pH was below 3, which was related to the high initial acidifying potential and large amounts of NO_3^- and SO_4^{2-} not involved in the neutralization reaction. The dominant cations in the sea fog water were Na^+ and NH_4^+. The primary anions in the sea fog water over the South China Sea were Cl^- and NO_3^-, while that over the North Pacific Ocean was mainly SO_4^{2-}, and ratios of the three fog water ions near the Donghai Island were similar. Ions in the sea fog water during the two events were mainly derived from marine aerosols, while the difference was that the first low-level sea fog airflow trajectory passed over Hainan Island. Therefore, the proportion of K^+ in the first sea fog was much higher than that in sea water and the second. Sulfate was the key to fog water nucleation, which made ion concentration in the sea fog water during the second event higher than that during the first. A decrease in average diameter during the first sea fog formation led to an ion concentration increase, while the average diameter of sea fog water during the second event was lower than that during the first, which corresponded with a moderate ion concentration increase.

Key words: northwestern South China Sea; sea surface fog; chemical properties; impact factors
CLC number: P426.4 **Document code:** A
Citation: HAN Li-guo, XU Feng, XU Jian-jun, et al. A Comparative Analysis of Chemical Properties and Factors Impacting Spring Sea Fog over the Northwestern South China Sea [J]. Journal of Tropical Meteorology, 2022, 28(3): 297-307, https://doi.org/10.46267/j.1006-8775.2022.023

1 INTRODUCTION

With accelerating global urbanization, air pollution has intensified, leading to a significant increase in pollutant content in fog, which poses a severe risk to human health and crop growth (Niu [1]; Niu et al. [2]; Ali et al. [3]). Since fog droplet condensation nuclei are aerosols, fog water chemical composition can reflect the aerosol composition of a particular area (Sasakawa and Uematsu [4]). Fog droplets can filter aerosols and acid gases from the atmosphere through a wet deposition mechanism (Sasakawa and Uematsu [5]; Lu et al. [6]), and can also be a carrier for chemical processes in the liquid phase (Pandis et al. [7]). Compared with rainwater, lower atmosphere fog water has higher pollutant concentration. Therefore, fog water chemical analysis is a crucial method to study contaminant long-range transport in the absence of rainfall and pollutant monitoring (Blas et al. [8]).

Acidification index (pH), electrical conductivity (EC), and total ion concentration (TIC) are the three most important parameters describing fog water chemistry (Yue [9]). Sea fog pH is lower than that of rainwater due to its high non-sea-salt sulfate ($nssSO_4^{2-}$) concentration (Jung et al. [10]; Kim et al. [11]). Nitric acid contributes significantly to sea fog acidification, as does dimethyl sulfide (DMS). As a dominant volatile organic sulfide in the ocean, DMS could also contribute to sea fog acidification (Sasakawa and Uematsu [5]; Sträter [12]). However, because pH results from the combined action of all anions and cations in sea fog water, it does not accurately reflect pollution. Fog water acid and alkaline

Submitted 2021-12-13; **Revised** 2022-05-15; **Accepted** 2022-08-15
Funding: National Key R&D Program of China (2018YFA0605604); Guangxi Key Research and Development Program (AB20159013); Strategic Priority Research Program of Chinese Academy of Sciences (XDA20060503); Key Area R&D Program of Guangdong Province (2020B0101130021); National Natural Science Foundation of China (41675136)
Biography: HAN Li-guo, Ph. D. candidate, primarily undertaking research on atmospheric physics and atmospheric environment.
Corresponding author: XU Feng, e-mail: gdouxufeng@126.com

content also need to be considered (Niu et al. [2]; Yue et al. [13]), such as their acidifying and neutralizing potentials (Tsuruta [14]; Fujita et al. [15]). Electrical conductivity reflects the ability of a medium to conduct electricity. It is directly related to dissolved ions, and usually has a good positive correlation with fog water total ion concentration (Li et al. [16]; Niu et al. [2]). The fog water chemical fraction in urban and mountainous areas (Wu et al. [17]; Wen et al. [18]; Niu et al. [2]) is charactered with SO_4^{2-}, Ca^{2+} or NH_4^+ dominant anions. However, that in sea fog at sea or on coastal shores or islands is with Cl^- and Na^+ dominant anions and cations (Yue et al. [19]; Yue et al. [20]; Xu et al. [21]). Moreover, correlation coefficients and ratios between fog-water ion concentrations combined with backward trajectory analysis can help to identify aerosol sources.

Fog-water ion concentration depends on aerosol and gas concentrations in the atmosphere and relates to the magnitude of removal efficiency (Niu [1]; Gilardoni et al. [22]; Straub [23]). Aerosol pollution levels are related to many factors, including air mass sources, long-range transport, weather systems, and meteorological parameters. Furthermore, removal efficiency needs to consider fog development strength, which can be expressed by the fog's microphysical parameter quantities. In previous studies, sea fog observations in the South China Sea mainly focused on coastal stations and islands. Sea fog boundary layer and microphysical characteristics were explored based on observations from the Bohe observatory in Maoming, Guangdong Province (Huang et al. [24]; Huang et al. [25]; Huang et al. [26]; Shen et al. [27]). Sea fog microphysical characteristics, chemical properties, and their relationships were investigated on Donghai Island, Guangdong Province (Xu et al. [28]; Yue et al. [19]; Zhao et al. [29]; Yue et al. [20]). Sea fog over the South China Sea mainly occurs within 2°–3° of latitude along the coast during February-April (Liu et al. [30]; Han et al. [31]). Underlying surface and land-sea differences make coastal and offshore sea fog chemical characteristics dissimilar, so sea fog observations should be conducted during the fog season and then compared to coastal fog observations.

2 METHODS

2.1 *Study area*

The South China Sea is an essential maritime transportation channel connecting the Indian and Pacific Oceans, and has a typical monsoon climate with sufficient water vapor conditions. In winter and spring, cold air from middle and high latitudes collides with warm and humid air from the nearby sea, often forming fog. Low visibility caused by sea fog severely affects road, marine and air transportation, and the combination of sea fog and airborne pollutants can also damage human health and reduce agricultural yields (Kasahara et al. [32]; Giulianelli et al. [33]; Niu et al. [2]). Therefore, sea fog is one of the most critical catastrophic weather events affecting economic development and human health. However, current sea fog studies are based on islands and coasts, and fog observation data (especially sea fog) is limited. There are also few reported studies based on sampling surface sea fog chemical characteristics.

Therefore, we installed sea fog observation instruments on a research vessel, which was sailed to a predetermined research area in the South China Sea, to observe and collect sea surface fog water samples. Then, we compared the physical and chemical characteristics and the influencing factors of sea surface fog. It would be a valuable contribution to sea fog research in China.

2.2 *Sea fog observation*

Our sea fog observation site was located in the northwestern part of the South China Sea (21.02° N, 110.86° E) (Fig. 1), about 50 km from Zhanjiang Port. The first sea fog observations were made during an obvious sea fog event that occurred from 21: 20 on March 10 to 6:40 on March 11, 2017. A total of nine fog water samples were collected during the event, and one rainwater sample was collected just after the end of it. A further five fog water samples were collected during the second, less lighter sea fog event that occurred from 03: 47 to 9:00 on March 12.

2.3 *Sampling and methods*

Fog micro-physical parameters, fog water samples, and regular meteorological elements were studied on board the scientific research vessel Haike 68. Fog microphysical parameters were measured with an FM-100 fog droplet spectrometer (DMT Company, United States), with a sampling frequency of 1 Hz. Variables included liquid water content, number concentration, and average droplet diameter. Fog water samples were sampled by a fog water collector every hour or one sample per two hours if fog water volume was low. The sampling container was repeatedly cleaned with high concentrations of alcohol and distilled water before sampling. After sampling, fog pH and conductivity were detected in situ. Meteorological variables, including temperature, humidity, air pressure, and wind speed, were measured at 1-min intervals. Ion detection was performed using an Intelligent Ion Chromatography-Professional IC 850 ion chromatograph (Metrohm Company, Switzerland), which automatically and simultaneously detects anions and cations.

2.4 *Calculation method*

pA_i is pH, assuming there is no sulfate type and nitrogen-containing acid neutralization in the atmospheric liquid water (Hara et al. [34]). In the calculation, the ratio of sulfate to sodium ions in sea water is taken as 0.12, and the ion concentration in the formula is μeq L^{-1}. The formula is as follows:

$$pA_i = -\log\left[\mathrm{nss}SO_4^{2-} + NO_3^-\right] \quad (1)$$

$$\mathrm{nss}SO_4^{2-} = SO_4^{2-} - \left(SO_4^{2-}/Na^+\right)_{\text{sea water}} \cdot Na^+ \quad (2)$$

The acidifying potential (AP) and neutralizing

potential (NP) are calculated via the following equations (Tsuruta et al. [14]). The ratio of calcium ions to sodium ions in sea water is taken as 0.044.

$$AP = \left[nssSO_4^{2-} + NO_3^- \right] \quad (3)$$

$$NP = \left[NH_4^+ + nssCa^{2+} \right] \quad (4)$$

$$nssCa^{2+} = Ca^{2+} - (Ca^{2+}/Na^+)_{\text{sea water}} \cdot Na^+ \quad (5)$$

Ion loading (IL) can be calculated using the following equation (Elbert et al. [35]), where ρ is the water density, IC(i) is the ionic concentration of the fog water species I (in μeqL^{-1}), and LWC is the liquid water content (in g m^{-3}), with an IL unit of μeqm^{-3}.

$$IL(i) = \frac{LWC \times IC(i)}{\rho} \quad (6)$$

2.5 *Data processing and quality control*

To facilitate analysis, an average of 1 min was used for all physical quantities, and data recorded during instrument abnormalities were eliminated and replaced with default values. A droplet spectrometer measured the droplet diameter from 1 to 50 μm and was divided into 20 steps. Since the measurement error of the first size bins (1−2 μm) was large, these data were discarded.

We estimated the ion balance deviation percentage during quality control of analyzing ion / cation concentration data in our samples (the ratio of the difference between the anion and cation concentrations to the sum). Based on the findings of Cini et al. [36] and Blas et al. [8], we considered that ion equilibrium was satisfied when the percentage difference of the ion balance (PDI) was between −5% and 35%, when H^+ was not detected, and when fog was acidic. Calculated results are shown in Table 1. Mean PDI for the 15 samples was 19.4%, with a standard deviation of 8.3%, and PDI ranged from 5.7 to 32%. Mean PDI for 9 samples in the first sea fog event was 16.2% with a standard deviation of 6.5%, PDI ranged from 5.7 to 26.8%, mean PDI for 5 samples in the second sea fog event was 27.1% with a standard deviation of 5.8%, and PDI ranged from 20.1 to 32%. The positive value indicates that the anion concentration is greater than that of cations, and the low pH of the second sea fog event compared to the first sea fog, led to a higher PDI. Data quality can also be checked by comparing the total cation, with the total anion concentration (Table 1, Degefie et al. [37]). Ion balance was in relatively good agreement between total anions and cations (mean value of 0.68 and standard deviation of 0.12). Therefore, data quality control based on both methods was within acceptable limits, which allowed for further ion concentration data analysis.

Table 1. Percentage deviation of ion balance (PDI), total ion concentration (TIC), and anion to cation ratio of fog water and rainwater in South China Sea fog.

	Sampling time	PDI	TIC	Anions/cations
Sea fog sample 1	3-10T21:20-22:00	19.3%	94859.6	0.68
	3-10T22:01-23:00	7.8%	6160.0	0.86
	3-10T23:01-00:00	5.7%	4490.2	0.89
	3-11T00:01-02:00	18.1%	20638.0	0.69
	3-11T02:01-03:00	26.8%	15952.8	0.58
	3-11T03:01-04:00	19.4%	19102.9	0.68
	3-11T04:01-05:00	19.0%	9079.6	0.68
	3-11T05:01-06:00	17.1%	7817.8	0.71
	3-11T06:01-07:00	12.5%	12324.0	0.78
Rain sample	3-11T07:01-10:00	9.9%	11940.8	0.82
Sea fog sample 2	3-12T03:47-05:00	32.0%	60905.2	0.52
	3-12T05:01-06:00	21.8%	16811.7	0.64
	3-12T06:01-07:00	20.1%	10675.5	0.66
	3-12T07:01-08:00	32.0%	20815.2	0.52
	3-12T08:01-09:00	29.8%	34345.9	0.54

3 CHEMICAL PROPERTIES OF SEA FOGS OVER THE SOUTH CHINA SEA

3.1 *Electrical conductivity and acidity indicators*

Electrical conductivity (EC) and total ion concentration (TIC) showed a relatively consistent trend, with a correlation coefficient of 0.97. Conductivity at the beginning of the two fog events was much higher than that during them, indicating that a large number of aerosols are dissolved in the fog water at the initial stage. Furthermore, conductivity at the end of the second fog event was much higher than that during it, corresponding to an increase in total ion concentration. Sea fog EC values ranged from 425 to 5400, with a

mean of 1965 μS cm^{-1}, close to the mean (1884) of the 2010 Zhanjiang Donghai Island fog event (Yue et al. [19]), and much higher than the mean (505) of the 2011 Zhanjiang Donghai Island fog event (Yue et al. [20]). Conversely, the sea fog total ion concentrations (in μeq L^{-1}) in 2010 were 23855.6 μeq L^{-1} and 34881.7μeq L^{-1}, respectively, which were much higher than that near the Donghai Island in Zhanjiang in 2011 (7653.9μeq L^{-1}).

Table 2. Conductivity (μS cm^{-1}) and acidity indicators of sea fog water and rainwater in the South China Sea.

	Sampling time	EC	pH	pAi	(pH-pAi)/pH	AP	NP	AP/NP	A_{lwc}
Sea fog sample 1	3-10T21:20-22:00	5400	3.07	4.4	−0.43	25309.5	11322.3	2.24	0.151
	3-10T22:01-23:00	541	3.50	3.23	0.08	1704.6	1147.1	1.49	0.304
	3-10T23:01-00:00	425	3.30	3.09	0.06	1239.3	1046.0	1.18	0.130
	3-11T00:01-02:00	1745	2.58	3.72	−0.44	5282.1	2742.3	1.93	0.060
	3-11T02:01-03:00	1595	2.56	3.79	−0.48	6194.9	2474.0	2.50	0.080
	3-11T03:01-04:00	1721	2.51	3.76	−0.50	5811.8	2511.7	2.31	0.050
	3-11T04:01-05:00	1063	2.76	3.51	−0.27	3238.5	1685.2	1.92	0.111
	3-11T05:01-06:00	938	2.86	3.41	−0.19	2549.2	1383.6	1.84	0.099
	3-11T06:01-07:00	1260	2.76	3.55	−0.29	3538.1	2088.7	1.69	0.038
Rain sample	3-11T07:01-10:00	810	4.05	3.3	0.19	2016.3	1172.2	1.72	−
Sea fog sample 2	3-12T03:47-05:00	4340	2.24	4.35	−0.94	22644.0	6137.6	3.69	0.021
	3-12T05:01-06:00	1901	2.52	3.77	−0.5	5953. 4	2747.0	2.17	0.025
	3-12T06:01-07:00	1394	2.65	3.58	−0.35	3803.0	1938.3	1.96	0.018
	3-12T07:01-08:00	1962	2.52	3.91	−0.55	8107.2	3027.2	2.68	0.012
	3-12T08:01-09:00	3220	2.31	4.1	−0.77	12651.3	4700.1	2.69	0.007

A_{lwc}: average of liquid water content

The acidity index (pH) is critical for characterizing fog water. Therefore, pH was examined for sea fog samples from the South China Sea for comparison with other regions, and to determine fog water acidity. Our results showed that pH of the first sea fog varied from 2.51 to 3.50 with a mean of 2.86, and pH of the second sea fog event varied from 2.24 to 2.65 with a mean of 2.45. The pH of both sea fog events was lower than those for coastal Donghai Island in 2010 (mean value of 5.2, Yue et al. [19]) and 2011 (mean value of 3.34, Yue et al. [20]).

Other parameters and methods have been proposed to determine fog water acidity. From the (pH-pAi)/pH results, the value for the first sea fog event ranged from −0.48 to 0.08, and the value for the second sea fog event from −0.94 to −0.35. The smaller positive value corresponds to the three extreme values of fog and rainwater pH; the negative value indicates that the concentration of other acids (e. g., hydrochloric acid, HCl) is greater than that of alkaline substances, and that H^+ from HNO_3 and H_2SO_4 did not participate in the neutralization reaction. The high concentration of NO_3^- and SO_4^{2-} ions during the two sea fog events (Table 3) and the mean values of (pH-pAi)/pH of −0.27 and −0.62 for the two sea fog events, respectively, indicate that a large amount of sulfate-type and nitrogen-containing acids did not undergo neutralization, resulting in the mean pH of below 3 in both sea fog events.

Tsuruta et al. [14] used acidifying potential (AP) and neutralization potential (NP) to analyze the magnitude of the contribution of acidic and alkaline substances when AP = NP, implying theoretically neutral water. For the first sea fog event, AP / NP ranged from 1.18 to 2.31, while for the second, it ranged from 1.96 to 3.69. The neutralization potential of the second sea fog event was weaker than that of the first, resulting in a lower pH. The AP of the initial sea fog event in the South China Sea was the largest, and the average AP of both fogs was 2.2 times NP, resulting in an average pH below 3.

3.2 *Fog water ion composition*

Ion concentration ratios of chloride (Cl^-), potassium (K^+), calcium (Ca^{2+}), and sodium (Na^+) in the North and South Pacific rainwater are relatively similar. In contrast, potassium ions account for a more significant proportion of South China Sea rainwater. Proportions of nitrate (NO_3^-) and ammonium (NH_4^+) in South China Sea rainwater are much higher than that in North and South Pacific rainwater, primarily because South China Sea rainfall occurs after the fog. The primary rainwater ions in different regions are chloride, and their ratios are much larger than those of nitrate and sulfate (SO_4^{2-}).

The main sea fog cations in different regions are

Table 3. Ratios between different ionic components and pH for sea fog and rain.

	Cl^-/ Na^+	SO_4^{2-}/ Na^+	NO_3^-/ Na^+	K^+/ Na^+	Ca^{2+}/ Na^+	Mg^{2+}/ Na^+	NH_4^+/ Na^+	NO_3^-/SO_4^{2-}	pH
South Sea fog 1	1.64	0.66	1.15	0.24	0.19	0.29	0.67	1.73	2.86
South Sea fog 2	1.69	1.23	1.31	0.15	0.10	0.27	0.79	1.06	2.45
South Sea rain	1.57	0.44	0.46	0.50	0.03	0.08	0.47	1.06	4.05
Donghai Island fog 2011[a]	1.46	1.81	1.79	0.12	0.32	0.30	–	0.99	3.34
North Pacific sea fog[b]	0.78	2.96	0.27	0.20	0.35	0.25	0.97	0.09	3.59
North Pacific rain[b]	1.25	0.26	0.08	0.02	0.07	0.25	0.01	0.31	4.54
South Pacific rain[b]	1.33	0.15	0.09	0.04	0.06	0.12	0.01	0.60	
Sea water[c]	1.17	–	–	0.02	0.04	0.23	–	–	–

a: (Yue et al. [20]); b: (Kim et al. [11]); c: (Keene et al. [38])

sodium and ammonium (see Yue et al. [20] for the 2011 Donghai Island sea fog episode). Average sodium and ammonium concentrations in the first South China Sea fog event were 3615 and 2423 μeq L^{-1}, respectively, while in the second, the values were 4395 and 3472 μeq L^{-1}, respectively. North Pacific fog has less anthropogenic influence based on low nitrate concentration. As a major contributor to aerosols over the North Pacific, the Taklimakan Desert imports large amounts of sulfate into the atmosphere each year and long-range transport to the North Pacific (Betzer et al. [39]; Gao et al. [40]; Zhuang [41]). Therefore, the high SO_4^{2-} concentration in the North Pacific sea fog is related to dust. Compared to North Pacific sea fog, where SO_4^{2-} is the primary ion, South China Sea fog is dominated by Cl^- and NO_3^-. Values of all these three ions in the Donghai Island are relatively similar. Average Cl^- and NO_3^-concentrations in the first South China Sea fog were 5941 and 4140 μeq L^{-1}, respectively, while in the second fog event, they increased to 7408 and 5736 μeq L^{-1}, respectively.

The Cl^- / Na^+ ratio in North Pacific Sea fog is lower than that in sea water (1.17), which may be due to HCl volatilization from sea salt particles leading to chloride depletion (Betzer et al. [39]; Collett et al. [42]; Kim et al. [11]). In contrast, the Cl^- / Na^+ ratio in sea fog in the South China Sea and Donghai Island is higher than that in sea water (1.17), suggesting that there may be other sources such as volcanic eruptions and anthropogenic burning that lead to excess droplet HCl (Gioda et al. [43]; Jung et al. [10]; Fu et al. [44]). The Mg^{2+}/Na^+ ratio in sea fog in different regions is close to that of sea water, indicating that Mg^{2+} is mainly from marine sources. The high calcium concentration is mainly from soil and sand (Millet et al. [45]; Ali et al. [46]). Although calcium to sodium ratio in sea fog in different regions is greater than the proportion in sea water, these ions are scarcer in South China Sea than in Donghai Island and North Pacific sea fogs. In the second South China Sea fog event, these ions were even scarcer than that in the first. This indicates that the influence of land-based sources on the two South China Sea fog events is less than those on the fogs over the North Pacific and Donghai Island. Compared with the Donghai Island and the first South

Table 4. Correlation analysis between different fog water ions in the northwestern South China Sea.

	pH	EC	F^-	Cl^-	NO_3^-	SO_4^{2-}	Na^+	NH_4^+	K^+	Mg^{2+}	Ca^{2+}
pH	1	−0.39	0.41	−0.13	−0.23	−0.42	−0.04	−0.26	−0.45	−0.01	0.18
EC		1	0.28	0.96**	0.98**	0.97**	0.94**	0.99**	0.21	0.93**	0.82**
F^-			1	0.46	0.34	0.34	0.51	0.38	−0.01	0.52	0.65*
Cl^-				1	0.99**	0.89**	0.99**	0.98**	0.19	0.99**	0.94**
NO_3^-					1	0.93**	0.97**	0.98**	0.19	0.97**	0.89**
SO_4^{2-}						1	0.87**	0.93**	0.10	0.86**	0.70**
Na^+							1	0.97**	0.05	0.99**	0.96**
NH_4^+								1	0.16	0.97**	0.89**
K^+									1	0.06	0.06
Mg^{2+}										1	0.97**
Ca^{2+}											1

** $P < 0.01$, * $P < 0.05$

China Sea fog event, the low calcium percentage of the second South China Sea sea fog event is related to aerosol differences between sea and land.

When the equivalent $NH_4^+/(SO_4^{2-}+NO_3^-)$ concentration ranges from 0.2 to 0.4, it is mainly influenced by marine sources (Zhuang [41]), and in the two South China Sea fog events it was 0.37 and 0.31, respectively. The NO_3^-/SO_4^{2-} reflects the relative contribution of the acidogenic precursors SO_2 and NO_x in fog water acidification, process of fog water, with a ratio greater than 1 for nitric acid type pollution. In the South China Sea, the sea fog pollutants were mainly of nitric acid type (Table 3).

In fog water samples, correlations between different chemical components (Table 4) can indicate whether they come from the same source, and whether they have the same chemical composition. pH did not correlate significantly with a single ion, while EC correlated better with higher ion concentrations. Potassium had a low correlation coefficient with other ions. F^- (the lowest ion concentration) had a correlation coefficient less than 0.7 with all other ions. Except for F^- and potassium, all other correlation coefficients between sodium, magnesium (Mg^{2+}), and chloride were > 0.99, indicating that the three elements are basically of the same origin, mainly from marine aerosols. Correlation coefficients between calcium and the above three ions were all > 0.94. Excessive calcium concentrations were mainly from soil and sand (Ali et al. [46]), and Ca^{2+}/ Na^+ levels in rainwater and sea fog during the second event in the South China Sea were close to those of sea water and lower than in sea fog in the Donghai Island. This indicates that Ca^{2+} in the second sea fog event mainly originated from marine aerosols, while in the first sea fog event was influenced to some extent by terrestrial aerosols. The correlation coefficient between NH_4^+ and NO_3^- and Cl^- was 0.98, and that between NH_4^+ and SO_4^{2-} was 0.93, and as pointed out by Aikawa et al. [47], NH_4^+ can exist as NH_4NO_3, $(NH_4)_2SO_4$, or NH_4HSO_4.

4 IMPACT FACTORS FOR WEATHER SYSTEMS AND MICROPHYSICAL PARAMETERS

4.1 *Weather systems and meteorological elements*

Air masses from different regions with different fog droplet condensation nuclei sources impact fog water and fog microphysical structure. Moreover, weather systems determine the dominant wind direction and air current movements from one region to another. Trajectory models can be used to effectively study air mass origin and horizontal transport (Blas et al. [8]). The first sea fog event occurred in the northwestern part of the South China Sea on 10−11 March 2017 (lasting about 10h). According to the Meteorological Information Comprehensive Analysis Process System (MICAPS) sea level pressure field data, the sea fog observation point was located in the southwest of the high pressure, one hour before the sea fog event occurred (20:00 10 March). Moreover, the high-pressure center was located at sea, and was a land high-pressure system moving to the sea (not shown). In the South China Sea, sea fog is stratospheric fog that forms when warm southward airflow moves to the cold sea surface to cool and reach saturation. Analysis of the backward airflow trajectory based on the Hybrid Single-Particle Lagrangian Integrated Trajectory (HYSPLIT4) model (Draxier and Hess [48]) (Fig. 1) showed that the first sea fog 1500m flow moved from the Central South Peninsula through the Beibu Gulf to the northwestern part of the South China Sea. The high pressure influenced the low-level flow and turned southward with height from the northeast. The low-level airflow moved from the South China Sea to the observation site via Hainan Island, and so marine aerosols and land mainly influenced the air mass along the track.

Although the wind speed during the second sea fog event was greater, and influenced by advection to some extent, the average temperature was significantly lower during the first sea fog event. Therefore, the second sea fog is advection, as well as advection radiation fog formed by the condensation of water vapor in the ground air layer due to radiative cooling by the sea surface. Low-level airflow came from southeast of the observation site on the ocean surface, and so marine aerosols mainly influenced the air mass. Affected by marine sources, and consistent with the results of marine aerosols observed by the South China Sea cruise in January 2010 (He [49]), the main anions in both South China Seafog events were Cl^- (Table 3), while observations of the South China Sea cruise in January 2003, affected by land sources caused by the northerly wind, show that SO_4^{2-} was the main ion (Zhang et al. [50]). Air temperature and air pressure had apparent opposite trends during the first advective fog event. In contrast, the second advective radiation fog changed little in temperature and had an apparent increasing trend in air pressure.

From a principal component analysis of first sea fog water, the two principal components explained 99.6 % of the total variance of fog water ion concentration (Table 5). The first factor had high loading on Cl^-, NO_3^-, SO_4^{2-}, Na^+, NH_4^+, Mg^{2+} and Ca^{2+}, which explained 86.8% of the variance. Combined with the backward trajectory (Fig. 1), correlations between different ions primarily originate from aerosols (Cl^-, Na^+, Mg^{2+} and Ca^{2+} all > 0.94, Table 4), and anthropogenic NO_3^- and NH_4^+ effects. The first factor represents a mixed marine and human source. The second factor only had a high load on K^+, which can be derived from biomass combustion in addition to sea salt, so this factor represents terrestrial sources. Therefore, biomass burning may explain why the proportion of K^+ in the first sea fog was much higher than in sea water (Table 3), and the high proportion of K^+ in the North Pacific sea fog near the Tsugaru Strait (Kim et al. [11];

Choi et al. [51]). The second sea fog water had only one factor, mainly from mixed marine and anthropogenic sources. The proportion of K^+ in the first fog event was greater than that in the second, which was related to land source. Variation in NO_3^-/SO_4^{2-} in the Haikou first six samples and the corresponding NO_2/SO_2 in the Haikou eight hours ahead (referring to the backward trajectory in Fig. 1a) of the first sea fog event were calculated using the water ion concentration during the first sea fog event and the hourly observed values of NO_2 and SO_2 in Haikou (data source: https://www. aqistudy. cn). The correlation coefficient between the two sequences was 0.72. Due to dimethyl sulfide oxidation produced by marine plankton, marine salt was mostly sulfate if it was not affected by terrestrial sources at sea. The proportion of SO_4^{2-} in the first sea fog event was low or related to terrestrial source impact.

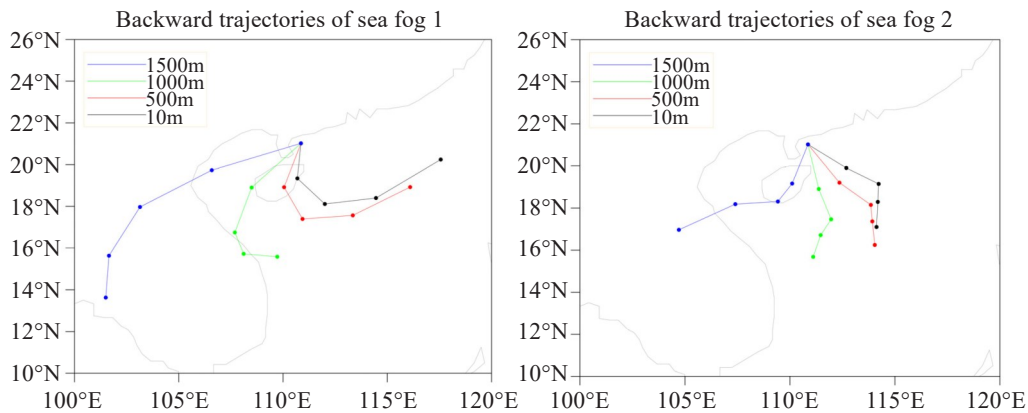

Figure 1. Backward airflow trajectories of the two sea fogs. Black, red, green, and blue curves indicate the 48-h backward airflow trajectories at 10, 500, 1000 and 1500m altitudes, respectively.

Table 5. Principal component analysis of sea fog water ions.

	Fog1		Fog2
Factor	1	2	1
Cl^-	**0.378**	0.053	**0.364**
NO_3^-	**0.378**	0.064	**0.361**
SO_4^{2-}	**0.378**	0.005	**0.361**
Na^+	**0.378**	−0.075	**0.36**
NH_4^+	**0.378**	0.056	**0.356**
K^+	0.025	**0.985**	**0.313**
Mg^{2+}	**0.378**	−0.08	**0.359**
Ca^{2+}	**0.377**	−0.087	**0.352**
Characteristic value	6.95	1.03	4.32
Variance contribution rate (%)	86.8	12.8	94.4

Factor loads greater than 0.3 are shown in bold.

4.2 *Microphysical parameters*

Atmospheric aerosol and liquid water content directly affect variation in total ion concentration in fog water, and so it is important to estimate air pollutants deposited through the fog. Therefore, we calculated the ion load (IL) to show the efficiency of nucleation and gas removal (Elbert et al. [35]). The ion loading is defined as the quantity of ions dissolved in the liquid phase in 1 m^3 of air.

The fog process is divided into four phases according to liquid water content variation (delimited by the black vertical dashed lines in Fig. 2): the first, second, and third liquid water content oscillations and the dissipation phase. The evolution of fog water NH_4^+, NO_3^- and SO_4^{2-} ion concentrations during the stratospheric fog event is shown in Fig. 2a. The explosive growth of sea fog began at 21: 20 (a rapid increase of LWC in Fig. 2c) and the first hour was fog water collection. Due to activation of droplets containing primary atmospheric pollutants (ammonium nitrate and ammonium sulfate), NH_4^+, NO_3^- and SO_4^{2-} concentrations in the fog water were the highest, and the number concentration and mean diameter also increased rapidly during this phase, indicating formation and activation of a large number of droplets on particles containing NH_4^+ , NO_3^- and SO_4^{2-} on the offshore surface. Compared to the hour at the beginning of the first oscillation period, concentrations of the three ions in the last two hours significantly dropped and were similar. Ion loadings were removed at different rates during this phase by wet deposition. As the reaction of sodium chloride and nitrate is faster than sulfate, the rate of change was in the order of $NO_3^- > NH_4^+ \approx SO_4^{2-}$. During the whole fog process, the increase (decrease) in the concentration of the three ions correlated well with the decrease (increase) in mean droplet diameter, indicating that sulfate, ammonium, and nitrate were present mainly in the smaller droplets. During the second oscillation phase, average diameter changed little in the first three hours, which indicates that competition for water by the smaller droplets led to restricted growth of the larger droplets. A similar concentration was maintained throughout much of the oscillation phase. Conversely, ion loading showed the same increasing-

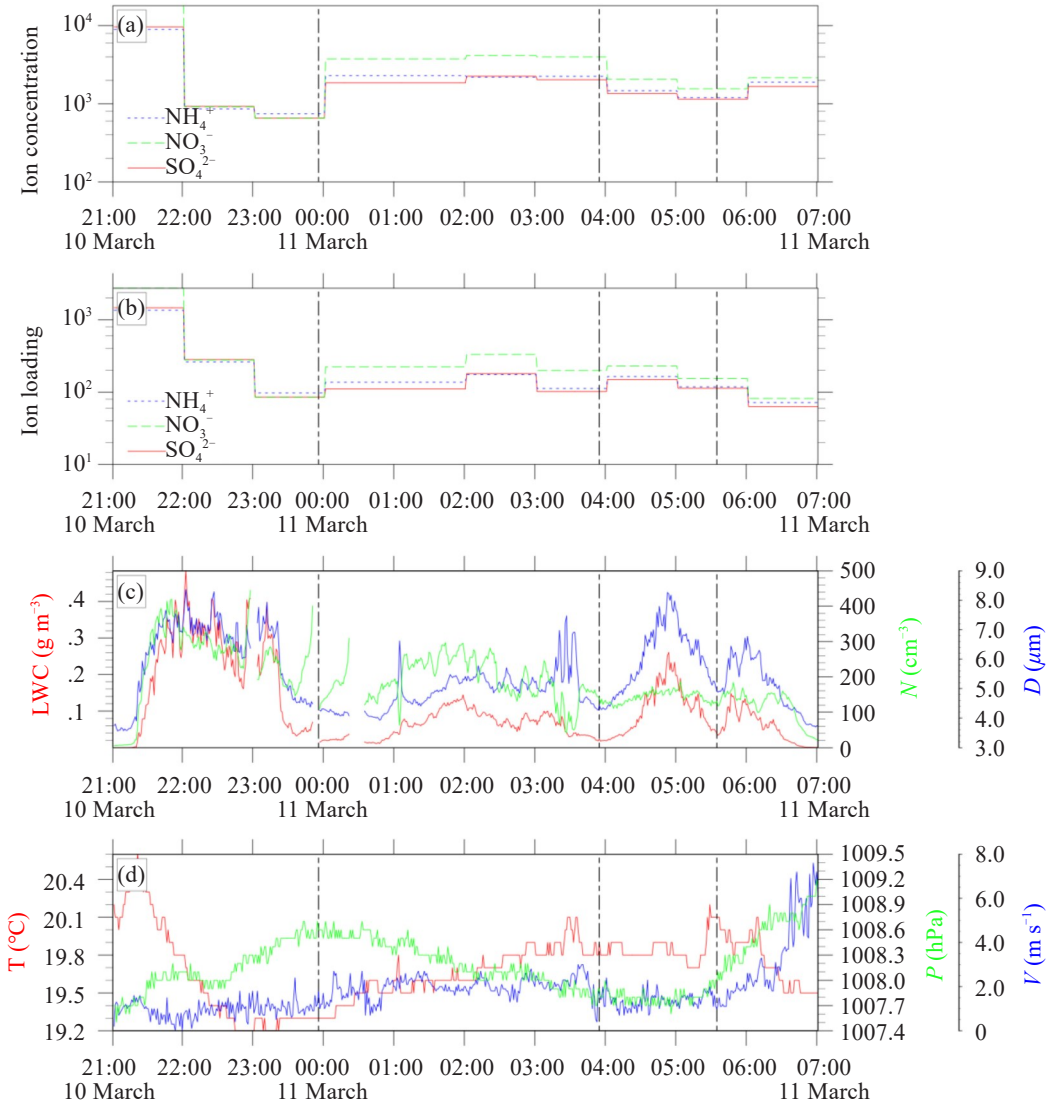

Figure 2. Sea fog ion concentration, ion loading, microphysical parameters, and conventional meteorological elements during the first sea fog event (red: SO_4^{2-}; green: NO_3^-; blue: NH_4^+).

decreasing oscillation as liquid water content, and the time mismatch was related to the time of fog water sampling. The slight ion concentration recovery during the dissipation phase corresponded to a decrease in liquid water content and mean diameter, and a weakening of the sedimentation scavenging effect. Ratios of NH_4^+, and NO_3^- to sodium in the rainwater samples after the sea fog episodes were about 47 and 6 times higher than those in the South and North Pacific, respectively, while the SO_4^{2-}/Na^+ ratio was less than twice that in the South and North Pacific (Table 2). Furthermore, the percentage of SO_4^{2-} during the second sea fog event was much higher than that during the first, corresponding to a greater ion concentration during the second sea fog event, indicating that sulfate may be the key to fog water formation.

Compared with the advective fogging process during the first fog event, liquid water content, mean diameter, and number concentration during the second fog even twere low, and it was a light fog. Trends in liquid water content and mean diameter correlated well, and concentration trends were relatively small. The ion concentration of the radiation fog showed an overall U structure. In the last two hours, ion concentration increased significantly, corresponding to decreasing liquid water content. The ion load showed a decrease followed by an increase, but the increased rate of change was much lower than the decreasing trend. The microphysical parameters of the fogging process (LWC, *D*, and *N* in Fig. 3b) had been oscillating at a high frequency, which was related to the rapid increase in wind speed. The oscillation brought water vapor and also inhibited fog development. As with the previously described advective fog, this fog water ion concentration and loading initiation phase successfully underwent a droplet activation process and wet deposition of the accumulated aerosol before the fog, corresponding to the maximum and maximum rate of change of the three ion concentrations and loadings. Compared with the average diameter and liquid water content of sea fog during the first sea fog event, those during the second sea fog event decreased while the average ion concentration increased.

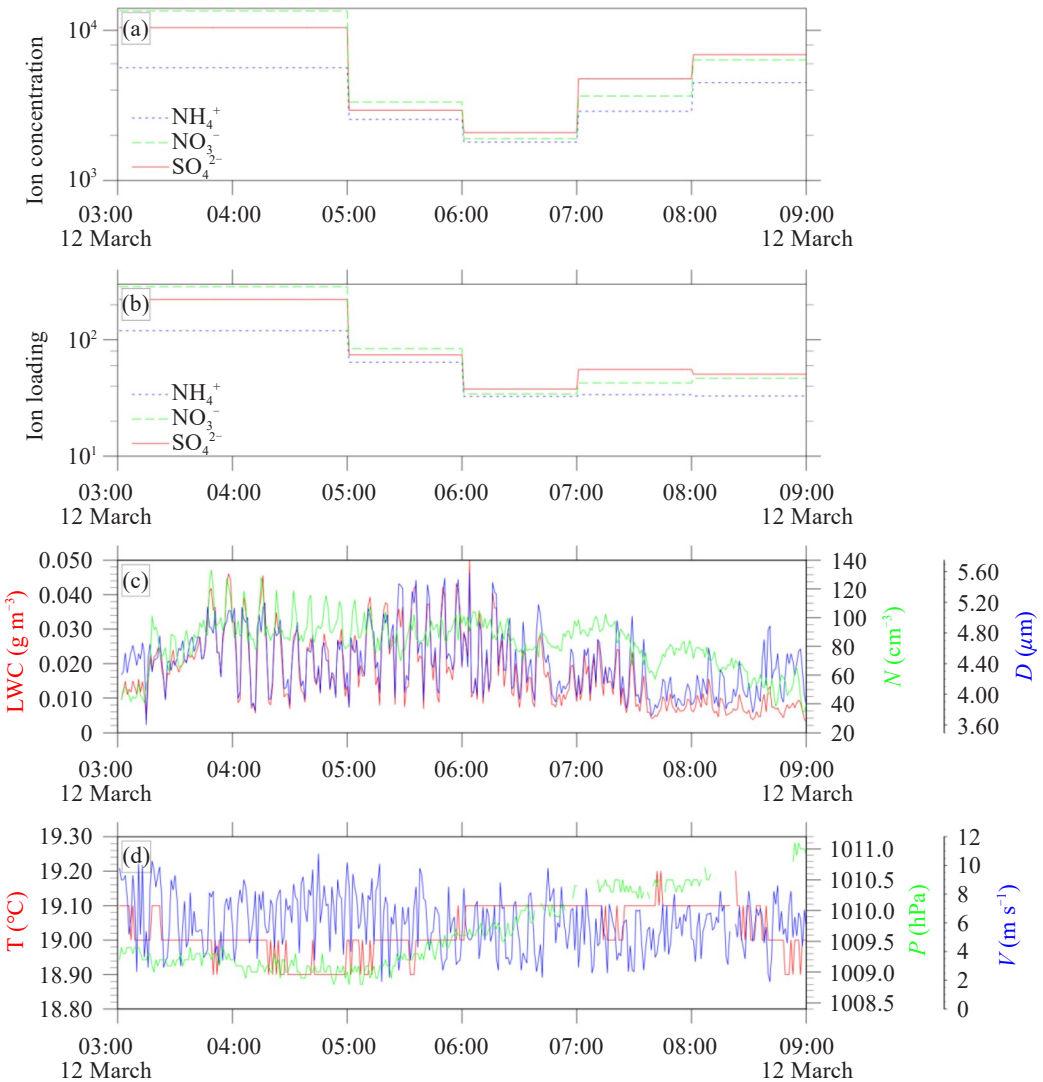

Figure 3. Sea fog ion concentration, ion loadings, microphysical parameters, and conventional meteorological elements during the second sea fog event (red: SO_4^{2-}; green: NO_3^-; blue: NH_4^+).

5 SUMMARY AND DISCUSSION

We analyzed the chemical properties and factors influencing fog and rainwater samples on the sea surface in the South China Sea, and compared sea fog along the coast of the South China Sea with those of other regions. Our results mainly indicated that:

(1) Sea fog water conductivity in the South China Sea showed a significant positive correlation with total ion concentrations. Initial AP during the two sea fog events was the largest, and the average was 2.2 times NP. A large amount of NO_3^- and SO_4^{2-} did not participate in the neutralization reaction, which led to the average pH of the sea fog during the two sea fog events below 3.

(2) The primary anion in the North Pacific Ocean was SO_4^{2-}, while sea fog anions in the South China Sea were mainly chloride and NO_3^-, and ratios of the three fog water ions near the Donghai Island were similar. Conversely, the dominant cations in sea fog water in different areas were Na^+ and NH_4^+. Ocean source mainly influenced water composition of the two South China Sea sea fog events. The two fog events over the South China Sea were different in that the sea fog during the first event had a low-level airflow trajectory passing through Hainan Island.

(3) The ratios of NH_4^+ and NO_3^- to Na^+ in rainwater samples after the first sea fog event were about 47 and 6 times, respectively, higher than those in the South and North Pacific samples. The ratio of SO_4^{2-} to Na^+ was less than two times those in the South and North Pacific samples, and the SO_4^{2-} ratio during the second sea fog event was much higher than during the first, corresponding to greater ion concentrations during the second sea fog event than that during the first, indicating that sulfate may be the key to fog water nucleation.

(4) The increase (decrease) in the concentration of the three ions during the first sea fog event correlated well with the decrease (increase) in mean diameter, indicating that sulfate, ammonium, and nitrate were present mainly in smaller droplets. Furthermore, in comparison with the diameter of sea fog during the first sea fog event, the decrease in the mean diameter of the

second sea fog event corresponded to the mean ion concentration increase.

There were some differences between the two sampling times and different stages during the sea fog events, suggesting that more targeted observations might be advantageous in the future.

REFERENCES

[1] NIU S J. Physical and Chemical Research of Fog [M]. Beijing: China Meteorological Press, 2014: 89-108 (in Chinese).

[2] NIU S J, LU C S, LÜ J J, et al. Advances in fog research in China [J]. Advances in Meteorological Science and Technology (in Chinese), 2016, 6: 6-19, https://doi. org / 10.3969/j.issn.2095-1973.2016.02.001

[3] ALI K, ACHARJA P, TRIVEDI D K, et al. Characterization and source identification of $PM_{2.5}$ and its chemical and carbonaceous constituents during Winter Fog Experiment 2015-16 at Indira Gandhi International Airport Delhi [J]. Science of the Total Environment, 2019, 662: 687-696, https://doi.org/10.1016/j.scitotenv.2019.01.285

[4] SASAKAWA M, UEMATSU M. Chemical composition of aerosol, sea fog, and rainwater in the marine boundary layer of the northwestern North Pacific and its marginal seas [J]. Journal of Geophysical Research: Atmospheres, 2002, 107(D24): ACH 17-1-ACH 17-9, https://doi. org / 10.1029/2001JD001004

[5] SASAKAWA M, UEMATSU M. Relative contribution of chemical composition to acidification of sea fog (stratus) over the northern North Pacific and its marginal seas [J]. Atmospheric Environment, 2005, 39(7): 1357-1362, https:// doi.org/10.1016/j.atmosenv.2004.11.039

[6] LU C S, NIU S J, TANG L L, et al. Chemical composition of fog water in Nanjing area of China and its related fog microphysics [J]. Atmospheric Research, 2010; 97: 47-69, https://doi.org/10.1016/j.atmosres.2010.03.007

[7] PANDIS S N, SEINFELD J H, PLINIS C. Chemical composition differences in fog and cloud droplets of different sizes [J]. Atmospheric Environment Part A General Topics, 1990, 24(7): 1957-1969, https://doi. org / 10.1016/0960-1686(90)90529-V

[8] BLAS M, POLKOWSKA Z, SOBIK M, et al. Fog water chemical composition in different geographic regions of Poland [J]. Atmospheric Research, 2010, 95(4): 455-469, https://doi.org/10.1016/j.atmosres.2009.11.008

[9] YUE Y Y. Observational Study on Microphysical Characteristics and Fog Water Chemical Composition of Sea Fog in Spring of South China Sea [D]. Nanjing: Nanjing University of Information Science and Technology, 2013: 1 (in Chinese).

[10] JUNG J, FURUTANI H, UEMATSU M, et al. Atmospheric inorganic nitrogen input via dry, wet, and sea fog deposition to the subarctic western North Pacific Ocean [J]. Atmospheric Chemistry and Physics, 2013, 13: 411-28, https://doi.org/10.5194/acp-13-411-2013

[11] KIM H J, LEE T, PARK T, et al. Ship-borne observations of sea fog and rain chemistry over the North and South Pacific Ocean [J]. Journal of Atmospheric Chemistry, 2019, 76: 315-326, https://doi. org / 10.1007 / s10874-020-09403-8

[12] STRÄTER E, WESTBELD A, KLEMM O. Pollution in coastal fog at Alto Patache, northern Chile [J]. Environmental Science and Pollution Research, 2010; 17: 1563-73, https://doi.org/10.1007/s11356-010-0343-x

[13] YUE Y Y, NIU S J, ZHANG Y, et al. Comparative analysis of sea fog water chemical composition in the coastal area of Donghai Island [J]. Acta Scientiae Circumstantiae, 2016, 36: 1573-80, https://doi. org / 10.13671/j.hjkxxb.2015.0768

[14] TSURUTA H. Acid precipitation in Eastern Asia [J]. Kagaku, 1989, 59: 305-315.

[15] FUJITA S, TAKAHASHI A, WENG J, et al. Precipitation chemistry in east Asia [J]. Atmospheric Environment, 2000, 34(4): 525-537, https://doi.org/10.1016/S1352-2310 (99)00261-7

[16] LI P F, LI X, YANG C Y, et al. Fog water chemistry in Shanghai [J]. Atmospheric Environment, 2011, 45(24): 4034-4041, https://doi. org / 10.1016 / j. atmosenv.2011.04.036

[17] WU D, LI F, DENG X J, et al. Study of the chemical characteristic of polluting fog in Guangzhou area in Spring [J]. Journal of Tropical Meteorology, 2009, 15: 68-72, https://doi.org/10.3969/j.issn.1006-8775.2009.01.011

[18] WEN B, YIN Y, QIN Y S, et al. Analyses of chemical characteristic in fog / cloud water and source at Mount Huangshan in summer 2009 [J]. China Environmental Science (in Chinese), 2012, 32: 2113-2122.

[19] YUE Y Y, NIU S J, ZHAO L J, et al. Chemical composition of sea fog water along the South China Sea [J]. Pure and Applied Geophysics, 2012, 169: 2231-2249, https://doi.org/10.1007/s00024-012-0486-4

[20] YUE Y Y, NIU S J, ZHAO L J, et al. The influences of macro - and microphysical characteristics of sea-fog on fog-water chemical composition [J]. Advances in Atmospheric Sciences, 2014, 31: 624-636, https://doi.org/ 10.1007/s00376-013-3059-2

[21] XU F, HAN L G, LÜ J P, et al. Analysis on microphysical and chemical characteristics of a sea fog on the sea surface in the northwestern south China sea [J]. Journal of Tropical Meteorology (in Chinese), 2019, 35: 596-603, https://doi.org/10.16032/j.issn.1004-4965.2019.054.

[22] GILARDONI S, MASSOLI P, GIULIANELLI L, et al. Fog scavenging of organic and inorganic aerosol in the Po Valley [J]. Atmospheric Chemistry and Physics, 2014, 14 (13): 6967-6981, https://doi. org / 10.5194 / acp-14-6967-2014

[23] STRAUB D J. Radiation fog chemical composition and its temporal trend over an eight year period [J]. Atmospheric Environment, 2017, 148: 49-61, http://dx.doi.org/10.1016/ j.atmosenv.2016.10.031

[24] HUANG H J, HUANG J, LIU C X, et al. Microphysical characteristics of the sea fog in Maoming area [J]. Acta Oceanologica Sinica (in Chinese), 2009, 31: 17-23.

[25] HUANG H J, LIU H N, JIANG W M, et al. Characteristics of the boundary layer structure of sea fog on the coast of Southern China [J]. Advances in Atmospheric Sciences, 2011, 28(6): 1377-1389, https:// doi.org/10.1007/s00376-011-0191-8

[26] HUANG H J, LIU H N, HUANG J, et al. Atmospheric boundary layer structure and turbulence during sea fog on the southern China Coast [J]. Monthly Weather Review, 2015, 143(5): 1907-1923, https://doi.org / 10.1175 / MWR-D-14-00207.1

[27] SHEN C, HUANG J, LIU S D, et al. Characteristics of quasi-periodic oscillations during sea fog events [J]. Journal of Tropical Meteorology, 2011, 17(1): 50-57.
[28] XU F, NIU S J, ZHANG Y, et al. Analyses on chemical characteristic of spring sea fog water on Donghai Island in Zhanjiang, China [J]. China Environmental Science, 2011, 31: 353-60.
[29] ZHAO L J, NIU S J, ZHANG Y, et al. Microphysical characteristics of sea fog over the east coast of Leizhou Peninsula, China [J]. Advances in Atmospheric Sciences, 2013, 30: 1154-1172, https://doi.org/10.1007/s00376-012-1266-x
[30] LIU S J, WU S A, LI W G, et al. Study on spatial-temporal distribution of sea fog in the South China Sea from January to March based on FY-3B sea fog retrieval data [J]. Journal of Marine Meteorology (in Chinese), 2017, 37(4): 85-90, https://doi. org / 10.19513 / j. cnki. issn2096-3599.2017.04.010
[31] HAN L G, LONG J C, XU F, et al. Decadal shift in sea fog frequency over the northern South China Sea in spring: Interdecadal variation and impact of the Pacific Decadal Oscillation [J]. Atmospheric Research, 2021, 265: 105905, https://doi. org / 10.1016 / j. atmosres.2021.105905
[32] KASAHARA M, AKASHI S, MA C J, et al. Fixation and chemical analysis of single fog and rain droplets [J]. Atmospheric Research, 2003, 65(3-4): 251-259, https://doi.org/10.1016/S0169-8095(02)00152-7
[33] GIULIANELLI L, GILARDONI S, TAROZZI L, et al. Fog occurrence and chemical composition in the Po valley over the last twenty years [J]. Atmospheric Environment, 2014, 98: 394-401, http://dx. doi. org / 10.1016/j.atmosenv.2014.08.080
[34] HARA H, KITAMURA M, MORI A, et al. Precipitation chemistry in Japan 1989-1993 [J]. Water Air amd Soil Pollution, 1995, 85: 2307-2312, https://doi.org / 10.1007 / BF01186178
[35] ELBERT W, HOFFMANN M R, KRAMER M, et al. Control of solute concentrations in cloud and fog water by liquid water content [J]. Atmospheric Environment, 2000, 34(7): 1109-1122, https://doi. org / 10.1016 / S1352-2310(99)00351-9
[36] CINI R, PRODI F, SANTACHIARA G, et al. Chemical characterization of cloud episodes at a ridge site in Tuscan Appennines, Italy [J]. Atmospheric Research, 2002, 61: 311-34, https://doi.org/10.1016/S0169-8095(01)00139-9
[37] DEGEFIE D T, EL-MADANY T S, HELD M, et al. Fog chemical composition and its feedback to fog water fluxes, water vapor fluxes, and microphysical evolution of two events near Paris [J]. Atmospheric Research, 2015, 164: 328-38, http://dx. doi. org / 10.1016 / j. atmosres.2015.05.002
[38] KEENE W C, PSZENNY A A P, GALLOWAY J N, et al. Sea-salt corrections and interpretation of constituent ratios in marine precipitation [J]. Journal of Geophysical Research: Atmospheres, 1986, 91: 6647-6658, https://doi.org/10.1029/JD091iD06p06647
[39] BETZER P R, CARDER K L, DUCE R A, et al. Long-range transport of giant mineral aerosol particles [J]. Nature, 1988, 336: 568-571, https://doi. org / 10.1038 / 336568a0
[40] GAO Y, ARUIMOTO R, ZHOU M Y, et al. Relationships between the dust concentrations over eastern Asia and the remote North Pacific [J]. Journal of Geophysical Research: Atmospheres, 1992, 97: 9867-9872, https://doi.org/10.1029/92JD00714
[41] ZHUANG G S. New theory of atmospheric aerosol and haze [M]. Shanghai: Shanghai Scientific and Technical Publishers, 2019: 30-199 (in Chinese).
[42] COLLETT J L, BATOR A, SHERMAN D E, et al. The chemical composition of fogs and intercepted clouds in the United States [J]. Atmospheric Research, 2002, 64(1-4): 29-40, https://doi.org/10.1016/S0169-8095(02)00077-7
[43] GIODA A, REYES-RODRÍGUEZ G J, SANTOS-FIGUEROA G, et al. Speciation of water - soluble inorganic, organic, and total nitrogen in a background marine environment: cloud water, rainwater, and aerosol particles [J]. Journal of Geophysical Research: Atmospheres, 2011, 116: D05203, https://doi.org/10.1029/2010JD015010
[44] FU J P, WANG B, CHEN Y, et al. The influence of continental air masses on the aerosols and nutrients deposition over the western North Pacific [J]. Atmospheric Environment, 2018, 172: 1-11, http://dx.doi.org/10.1016/j.atmosenv.2017.10.041
[45] MILLET M, SANUSI A, WORTHAM H. Chemical composition of fogwater in an urban area: Strasbourg (France) [J]. Environmental Pollution, 1996, 94: 345-54, https://doi.org/10.1016/S0269-7491(96)00064-4
[46] ALI K, MOMIN G A, TIWARI S, et al. Fog and precipitation chemistry at Delhi, North India [J]. Atmospheric Environment, 2004, 38: 4215-22, https://doi.org/10.1016/j.atmosenv.2004.02.055
[47] AIKAWA M, HIRAKI T, SHOGA M, et al. Chemistry of fog water collected in the Mt Rokko area (Kobe City, Japan) between April 1997 and March 2001 [J]. Water, Air, and Soil Pollution, 2005, 160: 373-393, https://doi.org/10.1007/s11270-005-3117-1
[48] DRAXIER R, HESS G D. An overview of the HYSPLIT_4 modeling system of trajectories, dispersion, and deposition [J]. Australian Meteorological Magazine, 1998, 47(4): 295-308.
[49] HE Y H. Composition and Source of Atmosphere Aerosol Water Soluble Ions over the China Coastal Seas [M]. Qingdao: Ocean University of China, 2011: 1 (in Chinese).
[50] ZHANG X Y, ZHUANG G S, GUO J H, et al. Characterization of aerosol over the Northern South China Sea during two cruises in 2003 [J]. Atmospheric Environment, 2007, 41: 7821-7836, https://doi. org / 10.1016/j.atmosenv.2007.06.031
[51] CHOI Y, RHEE T S, COLLETT J L, et al. Aerosol concentrations and composition in the North Pacific marine boundary layer [J]. Atmospheric Environment, 2017, 171: 165-172, https://doi. org / 10.1016 / j. atmosenv.2017.09.047

Citation: HAN Li-guo, XU Feng, XU Jian-jun, et al. A Comparative Analysis of Chemical Properties and Factors Impacting Spring Sea Fog over the Northwestern South China Sea [J]. Journal of Tropical Meteorology, 2022, 28(3): 297-307, https://doi. org / 10.46267/j.1006-8775.2022.023